Available online at www.sciencedirect.com
ScienceDirect
Ceramics International 36 (2010) 535–547
CERAMICS INTERNATIONAL
www.elsevier.com/locate/ceramint

The effect of natural dolomite admixtures on calcium zirconate–periclase materials microstructure evolution

Jacek Szczerba *, Zbigniew Pędzich

AGH, University of Science and Technology, Faculty of Materials Science and Ceramics, al. Mickiewicza 30, 30-059 Cracow, Poland

Received 28 November 2008; received in revised form 25 August 2009; accepted 7 September 2009
Available online 12 October 2009

Abstract

The reaction sintering mechanism of dolomite–zirconia mixtures was investigated using fine grounded dolomite raw material and zirconium powder. The used dolomite raw materials differed by the content of impurities (SiO_2, Al_2O_3 and Fe_2O_3 oxides). The microstructure evolution of MgO–$CaZrO_3$ and $CaZrO_3$ sintered materials was presented as a temperature function. One- and two-step firing processes of calcium raw materials powder mixed with chemically pure zirconium oxide were applied. The kinetics of reaction of $CaZrO_3$ synthesis was estimated by determining the ''free'' calcium oxide by chemical and XRD analysis. The densification process was evaluated by firing shrinkage, apparent density, pore diameter and pore size distribution measurements. The microstructure of sintered materials was observed by SEM. It was observed that $CaZrO_3$ synthesis was definitely finished at temperature of 1500 °C in the both applied ways of the synthesis (one- or two-step process). The only phase present in the model material synthesized from chemically pure reagents ($CaCO_3$ and ZrO_2) after firing at temperature of 1500 °C was calcium zirconate.

In the materials synthesized from natural dolomites and ZrO_2 two main phases were present—calcium zirconate and periclase. During firing of $CaZrO_3$–MgO materials at lower temperatures the presence of transient phases was detected (mainly ferrites and calcium aluminates, $4CaO{\cdot}Al_2O_3{\cdot}Fe_2O_3$ or $2CaO{\cdot}Fe_2O_3$). These phases disappeared at higher temperatures. This is probably related to the dissolution of impurities in the main phases of $CaZrO_3$–MgO.

The material obtained from the mixture of zirconium oxide and natural dolomite with the high impurities content has the highest densification level (~95% theoretical density of $CaZrO_3$–MgO) at 1500 and 1600 °C.

Keywords: Refractory materials; Dolomite; Periclase; Zirconia; Calcium zirconate; Synthesis

1. Introduction

Zirconia and calcium zirconate, despite their relatively high price, are very promising compound of high-refractory composites for the steel and cement industry. These phases introduced into refractory materials improve their properties, even if applied in relatively small amounts.

The advantages of zirconia are: high melting temperature, high density, good mechanical and thermomechanical properties and very good chemical resistance. Zirconium oxide with the melting temperature of 2700 °C has three polymorphs [1,2]. At low temperatures, the stable phase is a monoclinic one of the density 5.56 g/cm^3. During heating up to 1000–1200 °C it transforms into the tetragonal phase of the density 6.10 g/cm^3. This phase transformation is related to about 7 vol.% shrinkage, according to the decrease of specific volume of crystals. During cooling the reverse transformations occur. At temperatures higher than 2300 °C the cubic phase is stable. The polymorphism of zirconia hinders significantly creation of sintered bodies of this compound. From this point of view it is favourable to use zirconia solid solutions containing CaO, MgO and Y_2O_3 as stabilization agents.

The introduction of zirconia or calcium zirconate into magnesia or magnesia-spinel products leads to the significant improvement of the chemical resistance [3–6]. Zirconia can be added to magnesia products as a natural raw material: zircon ($ZrSiO_4$) and baddeleyit (ZrO_2). Another way to introduce zirconia could be the application of technical ZrO_2 products (stabilized or non-stabilized) or calcium zirconate.

In the ZrO_2–MgO system (Fig. 1), zirconia does not create chemical compounds with magnesia [7]. A permanent stabilization of zirconia to the cubic phase takes place at high

* Corresponding author. Tel.: +48 12 6172501.
E-mail address: jszczerb@uci.agh.edu.pl (J. Szczerba).

0272-8842/$36.00
doi:10.1016/j.ceramint.2009.09.025

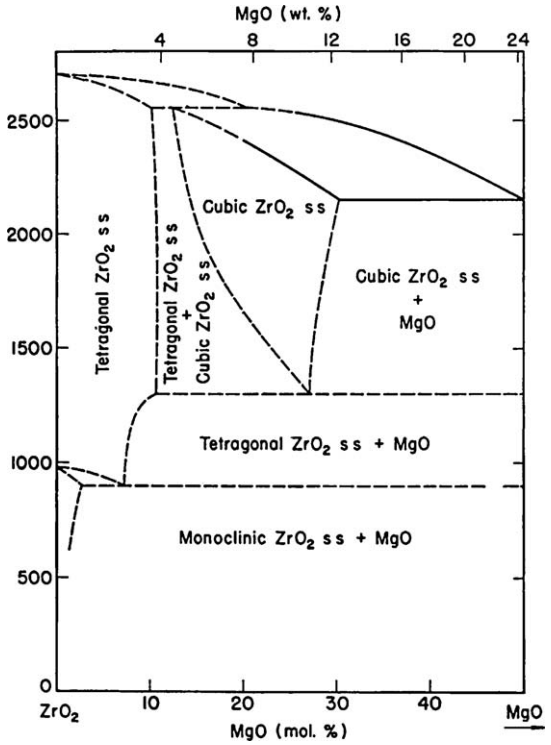

Fig. 1. The phase diagram in the MgO–ZrO_2 system [7].

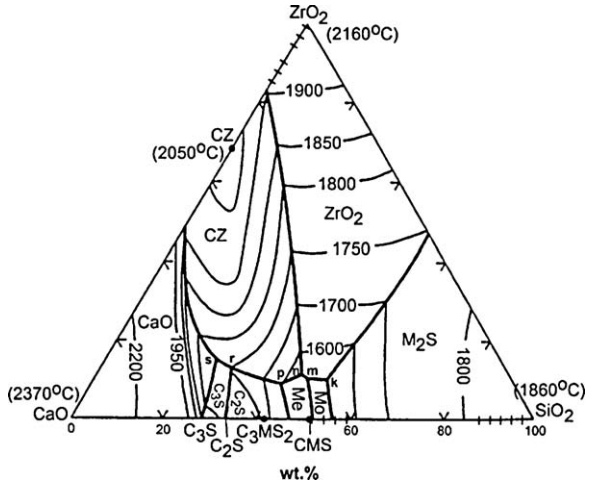

Fig. 2. The phase diagram in the MgO–CaO–ZrO_2–SiO_2 system for mixes containing 70% of MgO [15]. Composition of mixes was recalculated for 100% of CaO, ZrO_2 and SiO_2 content. The temperature at zero-variable points: k = 1485 °C, m = 1470 °C, n = 1475 °C, p = 1555 °C, r = 1710 °C, s = 1740 °C. Me – merwinite C_3MS_2, Mo – monticellite CMS.

temperatures for ∼16 mol.% of MgO. At lower temperatures the cubic zirconia phase is not stable phase and the MgO phase co-exists with tetragonal zirconia and zirconia phases.

In contact with CaO magnesia-spinel products (MSp) can create low-fusible calcium aluminates. It means that in contact with Portland clinker low-melting eutectics can appear. It is favourable for the creation of protective coat in the cement kiln. However, if the temperature of the lining of sintering zone in the rotary kiln exceeds the temperature of 1450 °C, the melting of MSp on the kiln surface can proceed. The presence of small amount of ZrO_2 in MSp products improves their chemical resistance [8–12]. This improvement is an effect of the formation of the high-refractory calcium zirconate phase [13].

Magnesia products with up to 5 wt.% of zirconia manufactured on the high purity magnesia base [3,5,6] contain periclase, stabilized zirconia or calcium zirconate and small amounts of silicates. The presence of zirconia phase improves the thermal shock resistance by generating small radial cracks on the surface of zirconia particles. These cracks are induced by the local volume changes related to phase transformation or $CaZrO_3$ (CZ) creation [9,14]. Additionally, diffusion processes at high temperatures leads to the ''direct bonding'' between periclase and zirconia. In the magnesia products with high CaO/SiO_2 molar ratio (>2) the $Ca_2[SiO_4]$ (C_2S) phase (possibly $Ca_2[SiO_4]O$ (C_3S)) and $CaZrO_3$ co-exist with MgO. In these products, the liquid phase can appear at the temperature exceeding 1700 °C (Fig. 2) [15]. Such products have very good thermomechanical properties [16].

If CaO/SiO_2 molar ratio is lower than 2, zirconia (with the presence of magnesia) co-exists with $Ca_2[SiO_4]$ and $Ca_3Mg[SiO_4]_2$ (C_3MS_2) or $Ca_3Mg[SiO_4]_2$ and $CaMg[SiO_4]$ (CMS) phases. In these products, the liquid phase appears at the temperature of 1555 °C or even lower. This product should be fired at the temperature of ∼1700 °C to assure the proper stabilization of zirconia with magnesia.

Magnesia products with the calcium zirconate addition are manufactured on the basis of sintered and/or fused magnesia with high CaO/SiO_2 molar ratio and sintered and/or fused calcium zirconate [3,4,13,17,18]. The synthetic calcium zirconate is introduced into the magnesia mass in a coarse- or fine-grained form, up to 20 wt.%. Calcium zirconate does not react with cement clinker components [19,20]. It effectively increases corrosion resistance of the material. $CaZrO_3$, during the work in the cement kiln, can dissolve in the liquid clinker phase and increase its viscosity [19]. This process limits infiltration of the cement clinker phase into the refractory.

Zirconia plays a similar role in dolomite products modification [14,21]. It improves not only the chemical resistance but also increases the resistance for hydration and thermal shock.

Nowadays, great interest is focused at the investigations on the utilization of limestone or dolomite in the mixes with zircon for refractory production [22–27].

The first way of manufacturing products with calcium zirconate (CZ) is based on the high-temperature reaction between zircon ($ZrSiO_4$) and calcium oxide in the mix [22,24]. Depending on the CaO/SiO_2 molar ratio in raw mixes, four types of products can be obtained (Table 1). The proportion of phases is described by CaO–SiO_2–ZrO_2 equilibrium triangle (Fig. 3). From the technical point of view belite- and alite-types of products are the most important.

The second way [23,25,26] of manufacturing products with magnesia–calcia–zirconia–silica (MCZS) is produced from dolomite and the zircon mix. During the high-temperature reaction between $ZrSiO_4$ and CaO products containing

Table 1
The types of calcia–zirconia (CZ) and magnesia–calcia–zirconia–silica (MCZS) materials depending on CaO/SiO_2 molar ratio.

CaO/SiO_2 (molar ratio)	Type	Type of material[a]	
		CZ	MCZS
1.5–2.0	Bagdadite	C_3S_2Z, C_2S, Z	–
2.0–3.0	Belite	C_2S, Z, CZ	–
3.0–4.0	Alite	C_2S, C_3S, CZ	M, C_2S, C_3S, CZ
>4.0	Alite-lime	C_3S, CZ, C	M, C_3S, CZ, C

[a] C – CaO; S – SiO_2; Z – ZrO_2; M – MgO.

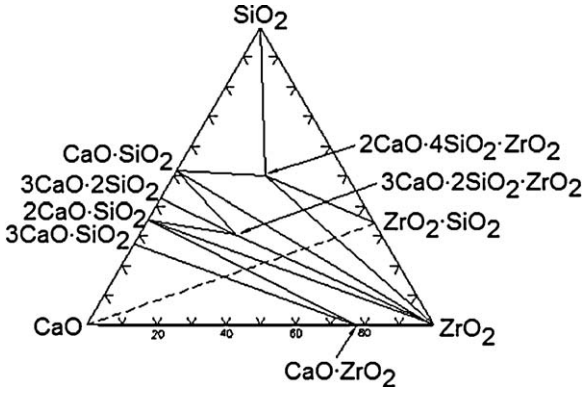

Fig. 3. The phase diagram in the $CaO–SiO_2–ZrO_2$ system [28].

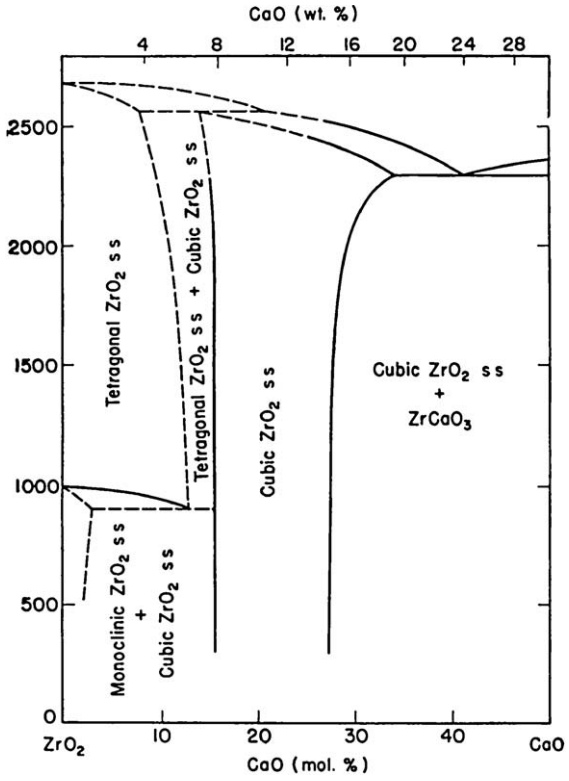

Fig. 5. The phase diagram in the $CaO–ZrO_2$ system [7].

periclase, calcium zirconate and high-refractory silicates are formed (Table 1).

According to the phase equilibrium in $MgO–CaO–ZrO_2–SiO_2$ system [15], the most favourable type of product has a high content of $Ca_2[SiO_4]$, or $Ca_2[SiO_4]$ co-exists with $Ca_3[SiO_4]O$ [23,26]. These products contain more than 40 wt.% of the silicate phase [24,25]. The $Ca_2[SiO_4]$ phase may exist in five polymorphs [29]. Four of them, (α, α'_H, α'_L and γ), are stable at different temperature ranges, the fifth one, (β), is unstable. The transformation of β-C_2S to γ-C_2S is related to 12% volume change, which can lead to the destruction of the material.

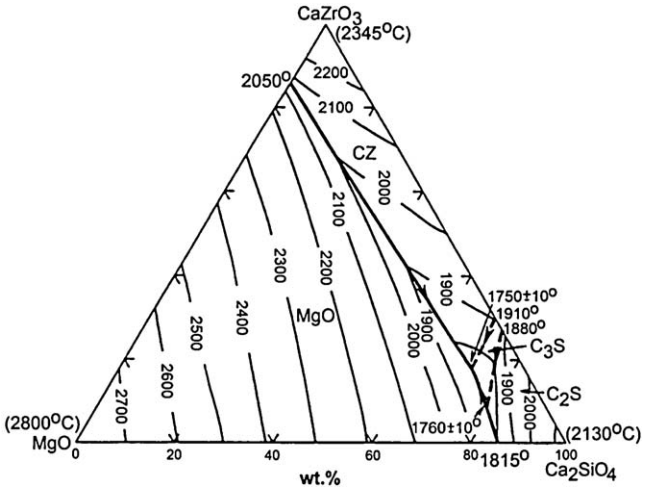

Fig. 4. The phase diagram in the $MgO–CaZrO_3–Ca_2SiO_4$ subsystem [15].

To a lesser extent, this phenomenon occurs in the $MgO–CaO–ZrO_2–SiO_2$ materials with a limited SiO_2 content. These materials can be obtained from the mixture of pure dolomite or limestone with zirconia. The basic compounds of these materials are high-refractory phases: periclase and calcium zirconate. The liquid phase in the $MgO–CaZrO_3$ system appears at the eutectic temperature of about 2050 °C (Fig. 4) [15].

As it comes from the phase diagram of $ZrO_2–CaO$, 15 mol.% CaO stabilizes the cubic ZrO_2 phase (Fig. 5) [7]. The only compound in this system is $CaZrO_3$ (CZ) with the melting point of 2345 °C [30] and stoichiometric CaO and ZrO_2 content.

The reaction of $CaZrO_3$ synthesis proceeds in the solid state. The dominating mass transfer mechanism is Ca^{2+} ions diffusion through a newly created compound [31]. Calcium zirconate synthesis starts at temperature ~900 °C and proceeds up to 1500 °C [19]. The creation of $CaZrO_3$ from CaO and ZrO_2 is assisted by the volume increase. The linear expansion can reach even 11% at temperature of 1500 °C. Calcium zirconate is chemically stable and does not show polymorphic transformations.

The paper presents the development of $MgO–CaZrO_3$ materials microstructure vs. temperature changes. Different manufacturing procedures (one- or two-step firing) were applied. Two types of dolomites with different content of SiO_2, Al_2O_3 and Fe_2O_3 impurities in the natural raw materials were used. The reaction was conducted in powder mixtures of dolomite and zirconia.

Table 2
The chemical composition of investigated materials.

Compound	Material			
	Dolomite I	Dolomite II	$CaCO_3$ (pure)	ZrO_2 (pure)
Loss on ignition	46.86	46.80	43.97	–
CaO	31.40	31.70	56.03	–
ZrO_2	–	–	–	100.00
SiO_2	0.04	0.50	–	–
MgO	21.67	19.70	–	–
Al_2O_3	0.03	0.10	–	–
Fe_2O_3	0.04	1.20	–	–

2. Experimental

The synthesis of magnesia–calcia–zirconia (MCZ) products was carried out with one- or two-step firing of dolomite and zirconia mixture. Two types of dolomite with different content of natural admixtures were mixed with pure synthetic zirconia (described as DI material and DII material, respectively).

For comparison, the reaction of $CaZrO_3$ synthesis was also carried out with high purity calcium carbonate and zirconium oxide (W material).

Table 2 presents the chemical composition of the raw materials. The total amount of SiO_2, Al_2O_3 and Fe_2O_3 admixtures in the dolomite I was about 0.1 and 1.8 wt.% in the dolomite II.

First of all, the size of a natural materials grains was reduced below 0.063 mm. Consequently, the mixtures of dolomite powder or pure chemical $CaCO_3$ with pure chemical zirconia were compiled in the proportion giving CaO to ZrO_2 ratio corresponding to $CaZrO_3$ stoichiometry. After homogenization by mechanical mixing of masses, pellets with 10 mm in diameter were pressed at 120 MPa.

Firing was carried out in two ways. During the one-step process, pellets were heated up to maximum temperature of 1000, 1100, 1200, 1300, 1400, 1500 and 1600 °C. The soaking time at maximum temperature was 120 min; the cooling stage proceeded together with the furnace.

The two-step process consists of heating up to 1200 °C, soaking for 60 min and cooling with the furnace. After this stage, the samples were ground to the grain size lower than 0.063 mm and again pressed under 120 MPa. Consequently, the samples were fired at temperature of 1400, 1500 or 1600 °C with 120 min soaking time and cooled with the furnace. The samples achieved in this way were described as (DI/2, DII/2 and W/2).

The evaluation of $CaZrO_3$ formation was performed by two methods. The first one was measuring "free" calcia (CaO_{free}), using the chemical method consist in reaction between ethyl glycol and "free" CaO at temperature range 65–75 °C and consequently determining of Ca ions amount by titration. The second method was the estimation of the phase composition by the XRD analysis.

The densification degree was estimated by linear shrinkage of sample diameter measurements and by determination of bulk

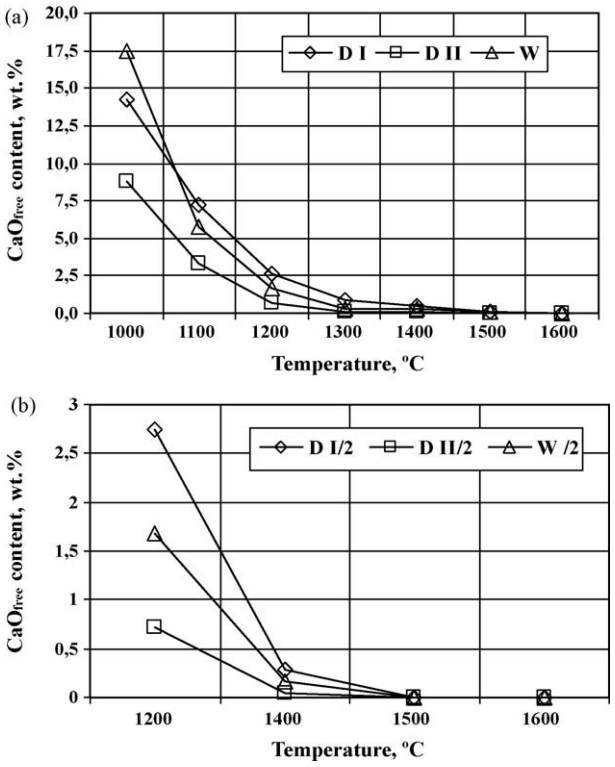

Fig. 6. The "free" calcium oxide (CaO_{free}) changes vs. firing temperature. (a) The one-step firing with 120 min soaking time. Materials synthesized from dolomite I – DI, dolomite II – DII, calcium carbonate – W. (b) The two-step firing with 120 min soaking time. Materials synthesized from dolomite I – DI/2, dolomite II – DII/2, calcium carbonate – W/2.

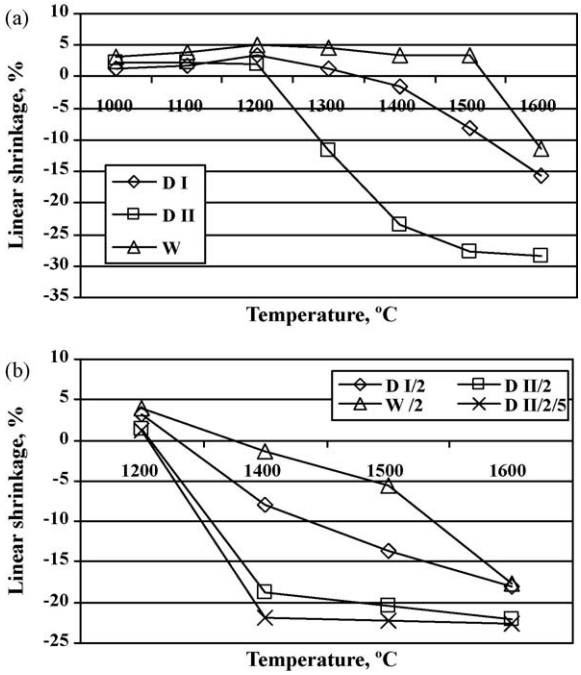

Fig. 7. The linear shrinkage of materials fired in one-step (a) or two-step (b) processes vs. firing temperature.

density. Additionally, the pore size distribution was measured using mercury porosimetry.

The microstructure of samples was investigated by SEM, accompanied by the EDS chemical analysis in microareas.

3. Results and discussion

Fig. 6 presents changes of the ''free'' CaO content in the products vs. firing temperature. Independently of the type of firing and its maximum temperature, the DII product contains lower amount of ''free'' CaO. The level of 0.1% CaO was reached for DII material at temperature of 1300 °C.

The same level in DI and W samples was reached after firing at temperature of 1500 °C. For these materials the amount of CaO decreased with the firing temperature, in a similar way.

For one-step firing the amount of ''free'' CaO decreased to zero at temperature of 1500 °C for DII material and at temperature of 1600 °C for DI and W materials.

The products obtained through two-step firing at temperature of 1400 °C had a small amount of ''free'' calcium oxide – 0.04% for DII/2, 0.28% for DI/2 and 0.16% for W. In the samples manufactured at temperatures of 1500 and 1600 °C the ''free'' CaO was not detected.

XRD analysis showed that the main phase of all materials after one-step firing at 1000 °C was calcium zirconate (Table 3).

In W material (mixture of $CaCO_3$ and ZrO_2), after one-step process, up to temperature of 1200 °C, calcium stabilized

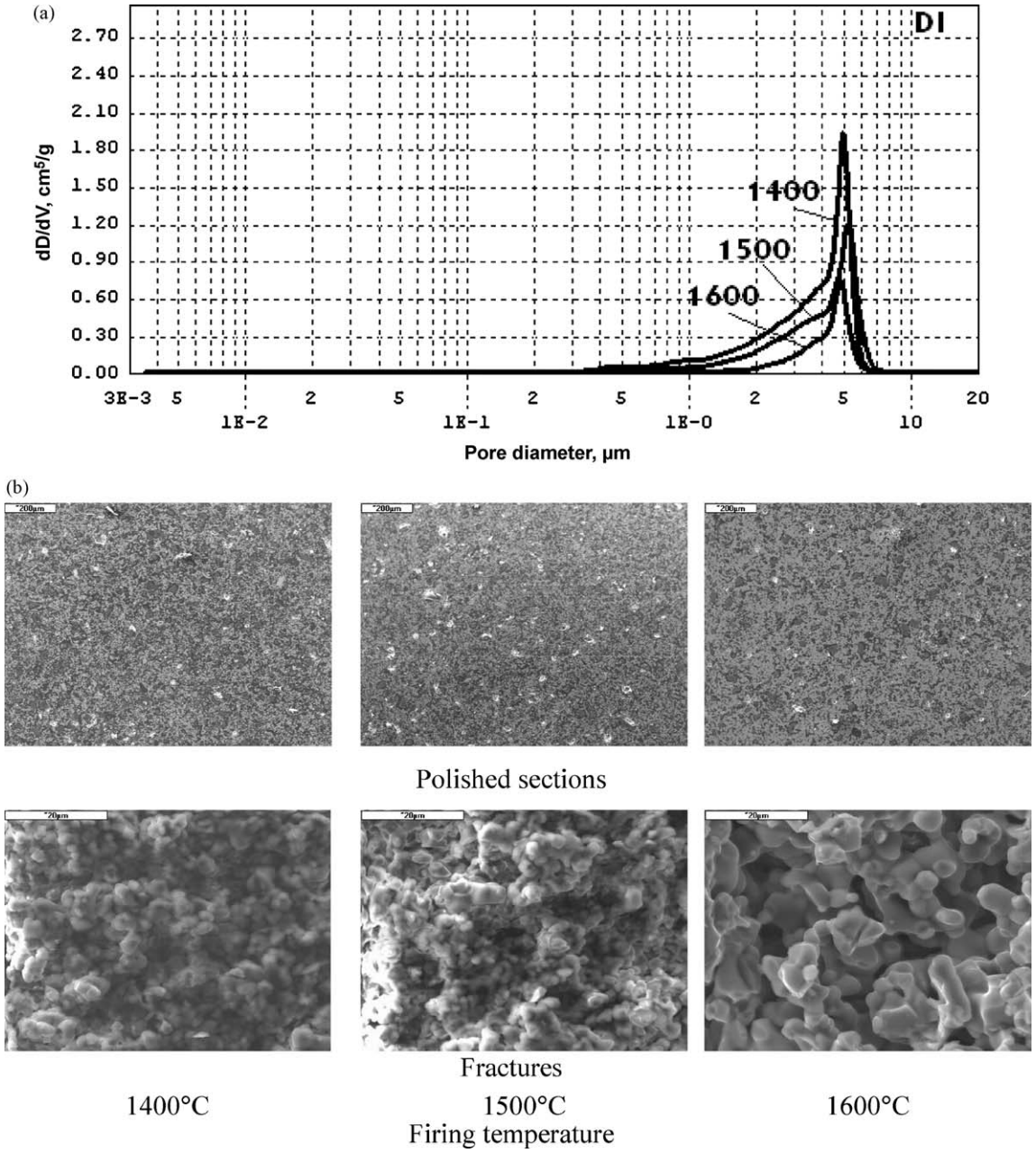

Fig. 8. Pore size distribution (pore frequency curve) (a) and SEM images of microstructure (b) of DI material. Bright oval grains – calcium zirconate; dark grey grains – periclase and dark spots – pores.

Table 3
The phase composition of DI, DII and W materials after one-step firing.

Firing temperature (°C)	Phases identified in the material listed in decreasing order		
	DI	DII	W
1000	$CaO{\cdot}ZrO_2$; MgO; Ca–ZrO_2; CaO	$CaO{\cdot}ZrO_2$; MgO; Ca–ZrO_2; CaO; $4CaO{\cdot}Al_2O_3{\cdot}Fe_2O_3$	$CaO{\cdot}ZrO_2$; Ca–ZrO_2; CaO;
1100	$CaO{\cdot}ZrO_2$; MgO; Ca–ZrO_2; CaO	$CaO{\cdot}ZrO_2$; MgO; Ca–ZrO_2; CaO	$CaO{\cdot}ZrO_2$; Ca–ZrO_2; CaO;
1200	$CaO{\cdot}ZrO_2$; MgO; Ca–ZrO_2; CaO	$CaO{\cdot}ZrO_2$; MgO; Ca–ZrO_2; CaO	$CaO{\cdot}ZrO_2$; Ca–ZrO_2; CaO;
1300	$CaO{\cdot}ZrO_2$; MgO; Ca–ZrO_2; CaO	$CaO{\cdot}ZrO_2$; MgO; Ca–ZrO_2; CaO	$CaO{\cdot}ZrO_2$
1400	$CaO{\cdot}ZrO_2$; MgO; Ca–ZrO_2 (traces)	$CaO{\cdot}ZrO_2$; MgO; Ca–ZrO_2	$CaO{\cdot}ZrO_2$
1500	$CaO{\cdot}ZrO_2$; MgO	$CaO{\cdot}ZrO_2$; MgO; Ca–ZrO_2; $2CaO{\cdot}Fe_2O_3$	$CaO{\cdot}ZrO_2$
1600	$CaO{\cdot}ZrO_2$; MgO	$CaO{\cdot}ZrO_2$; MgO; Ca–ZrO_2 (traces)	$CaO{\cdot}ZrO_2$

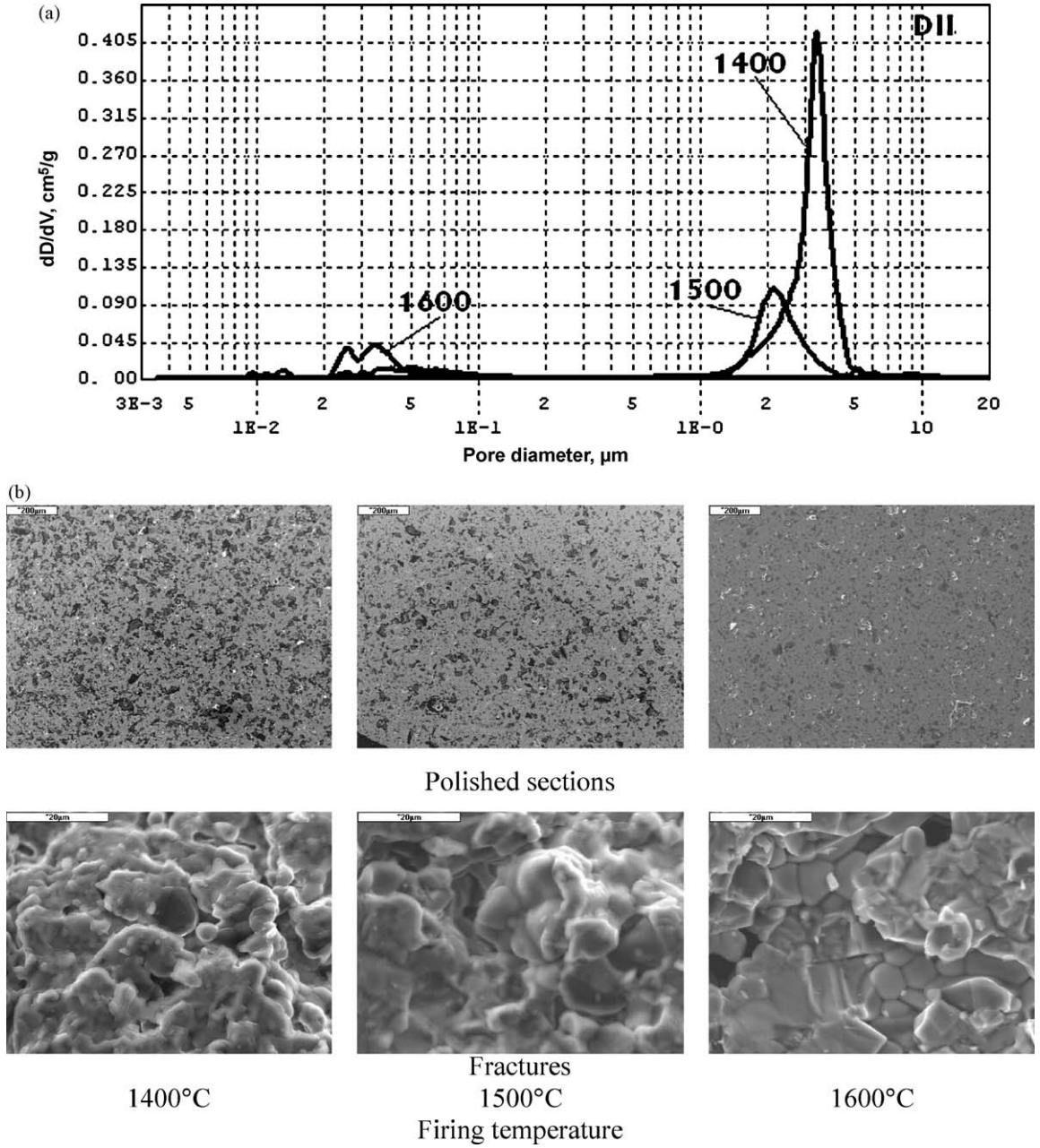

Fig. 9. Pore size distribution (pore frequency curve) (a) and SEM images of microstructure (b) of DII material. Bright oval grains – calcium zirconate; dark grey grains – periclase and dark spots – pores.

zirconia (identified as $Ca_{0.15}Zr_{0.85}O_{1.85}$) and ''free'' calcium oxide were identified. In the samples fired at temperature of 1300 °C (and at higher temperatures) XRD analysis detected only $CaZrO_3$ (Table 3). The ''free'' CaO content measured by the chemical method was 0.34% (at 1300 °C).

In DI and DII materials after one-step firing the main identified phase was calcium zirconate assisted by periclase (MgO) and calcium stabilized zirconia. The amount of the last mentioned phases decreased with temperature.

''Free'' CaO in DI material was detected up to 1300 °C. Its content measured by the chemical method was 0.84% (at 1300 °C). In DII material ''free'' CaO was detected up to 1200 °C and amounted to 0.67%. The phase composition of DI and DII materials after one-step firing at temperature of 1400 °C showed, except the main phases ($CaZrO_3$ and MgO), traces of CaO stabilized zirconia.

In DI material after one-step firing at temperatures of 1500 and 1600 °C exclusively, calcium zirconate and periclase were recognized (Table 3).

The products obtained through the one-step firing of DII material in the temperature range of 1000–1500 °C contained traces of transition ferrite phase – calcium ferrite, $Ca_2Fe_2O_5$ ($2CaO{\cdot}Fe_2O_3$), with the melting point of 1449 °C [32] or calcium ferrite-aluminate – brownmillerite Ca_2AlFeO_5

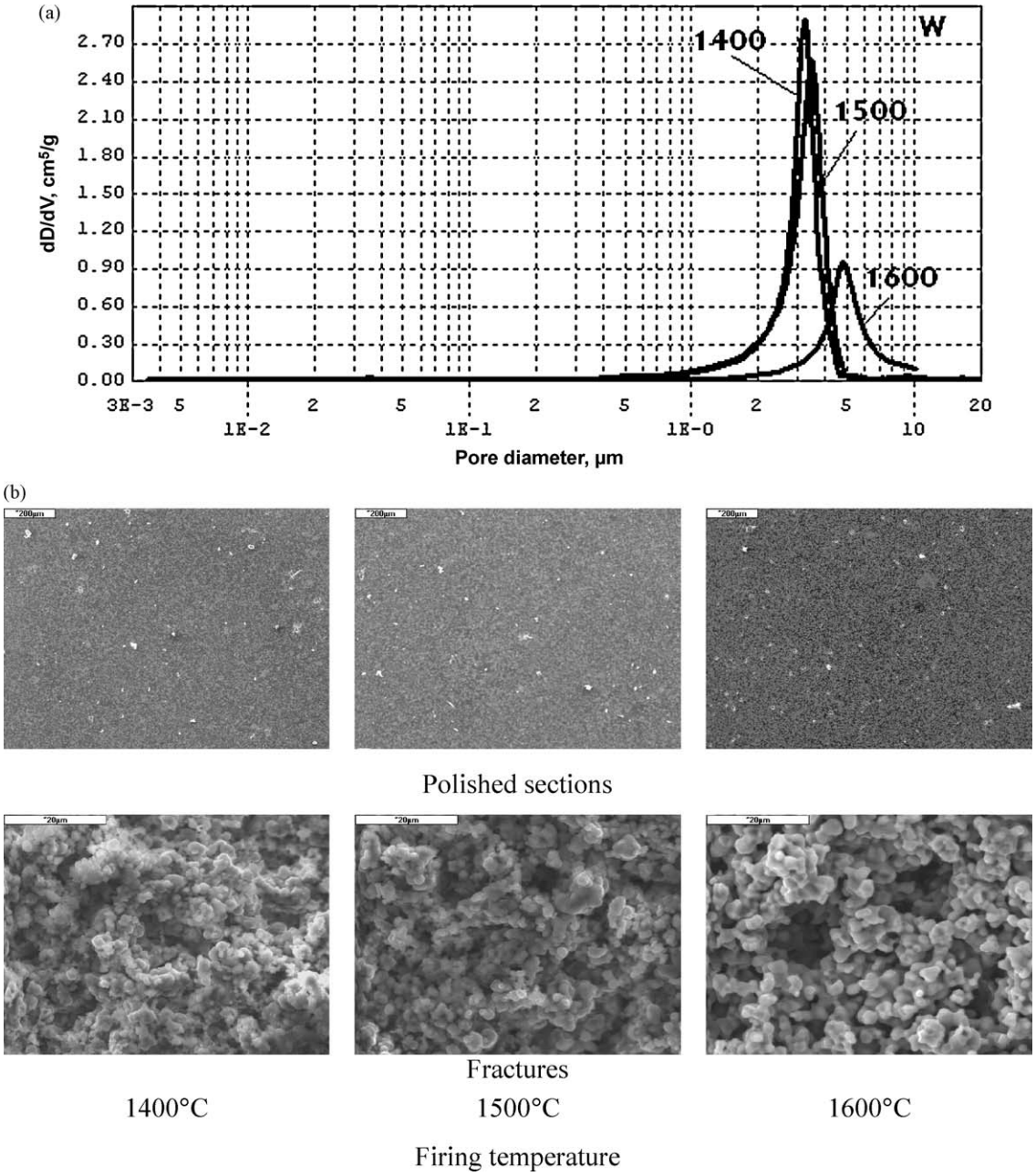

Fig. 10. Pore size distribution (pore frequency curve) (a) and SEM images of microstructure (b) of W material. Bright oval grains – calcium zirconate; dark grey grains – periclase and dark spots – pores.

($4CaO{\cdot}Al_2O_3{\cdot}Fe_2O_3$) with the melting point of 1415 °C [33]. The silicon oxide present in natural dolomite II in an amount of 0.5% could create (together with CaO) calcium silicates $Ca_2[SiO_4]$ with the melting point of 2130 °C and $Ca_2[SiO_4]O$ with the incongruent temperature of 2070 °C [34].

As it could be derived from the phase diagram of CaO–MgO–ZrO_2–SiO_2 system, in the material with high CaO/SiO_2 (>2) ratio, MgO could be accompanied by $Ca_3[SiO_4]O$ (with a possible presence of $Ca_2[SiO_4]$ and $CaZrO_3$). The liquid phase could appear in this material at the temperatures above 1700 °C (Fig. 2) [15]. The appearance of the liquid phase below this temperature is related to the presence of ferrites and calcium aluminates. For CaO–MgO–Al_2O_3 system, in MgO–$C_{12}A_7$–C_3A co-stability triangle, the liquid phase appeared at 1321 °C as eutectic point [35].

In the M–C_2S–C_4AF system containing brownmillerite (C_4AF), the liquid phase appeared at temperature of 1320 °C [33]. In DII material after firing at temperature of 1600 °C traces of the stabilized zirconia were detected (apart from the main phases – periclase and calcium zirconate) (Table 3).

The decay of ferrite and aluminates transition phases at higher firing temperatures is probably related to the dissolution of little Fe_2O_3, Al_2O_3 and SiO_2 into the main phases of $CaZrO_3$–MgO material [36,37].

After the first firing at temperature of 1200 °C during two-step process, the ''free'' CaO content was 2.74, 0.72 and 1.68

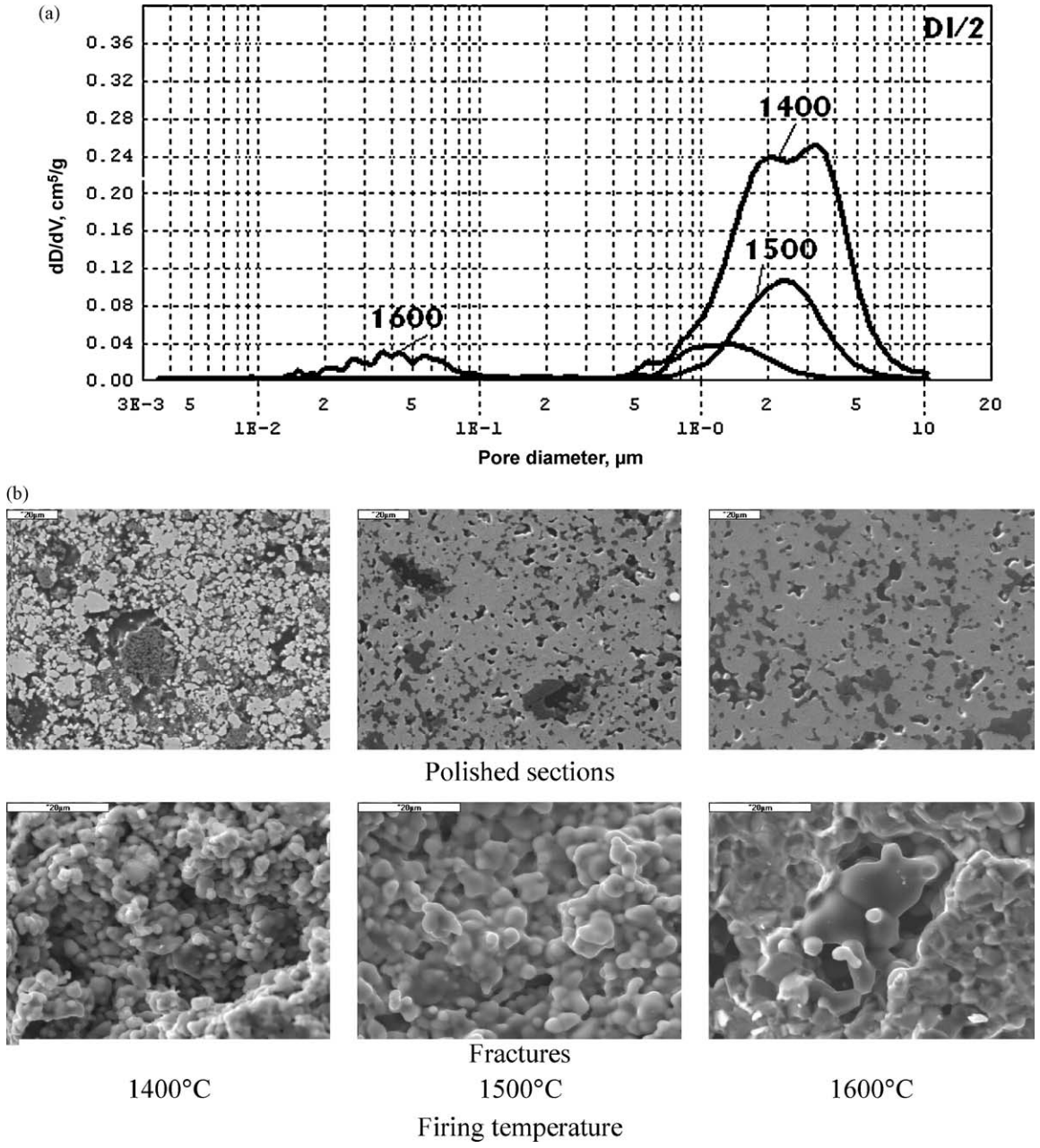

Fig. 11. Pore size distribution (pore frequency curve) (a) and SEM images of microstructure (b) of DI/2 material. Bright oval grains – calcium zirconate; dark grey grains – periclase and dark spots – pores.

for DI/2, DII/2 and W/2 materials, respectively (Fig. 6). The materials obtained through the second step of firing at temperatures of 1500 and 1600 °C contained no ''free'' CaO. The phase composition of the materials fired at temperatures of 1400, 1500 and 1600 °C (Table 4) was the same as for the materials obtained in one-step firing (Table 3).

''Free'' CaO measurements and phase composition analysis show that the synthesis of $CaZrO_3$ was finished at temperature of 1500 °C in all investigated systems (Fig. 6).

During the one-step processing, DI material (up to 1300 °C), DII material (up to 1200 °C) and W material (up to 1500 °C) showed small volume increase, with high shrinkage at higher temperatures (Fig. 7). The maximum linear expansion of materials was at 1200 °C: 3.4% for DI material, 2.0% for DII material and 5.0% for W material.

DII material after firing from 1300 °C and higher showed significant shrinkage (Fig. 7). This phenomenon was probably an effect of the liquid phase appearance which intensified the sintering process. This phase was formed of CaO, Fe_2O_3, Al_2O_3 and SiO_2. The amount of these oxides in the natural dolomite II was 1.8 wt.% (see Table 2). As it was shown by XRD analysis

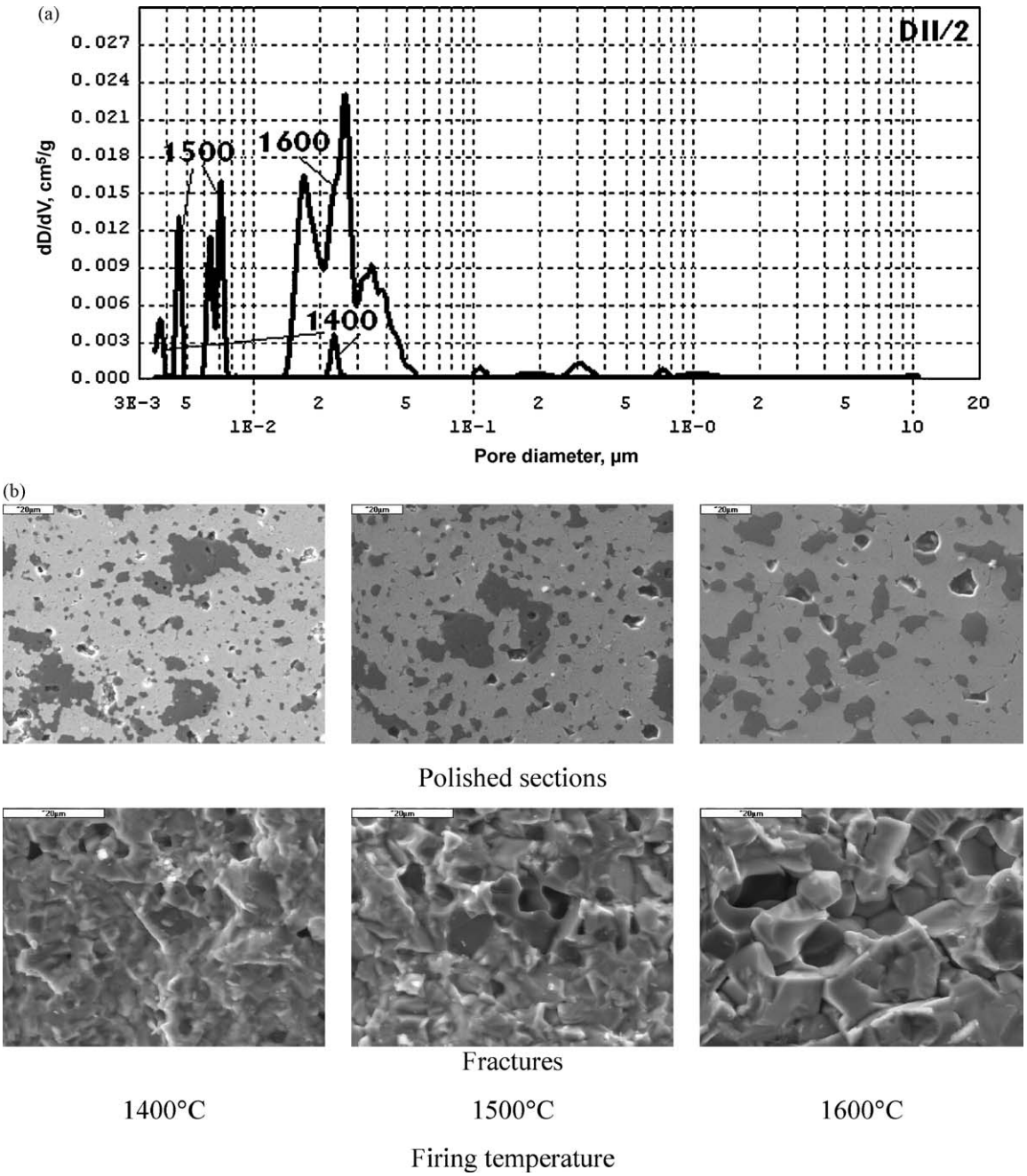

Fig. 12. Pore size distribution (pore frequency curve) (a) and SEM images of microstructure (b) of DII/2 material. Bright oval grains – calcium zirconate; dark grey grains – periclase and dark spots – pores.

Table 4
The phase composition of DI/2, DII/2 and W/2 materials after two-step firing.

Firing temperature (°C)	Phases identified in the material listed in decreasing order		
	DI/2	DII/2	W/2
1400	$CaO{\cdot}ZrO_2$; MgO; Ca–ZrO_2 (traces)	$CaO{\cdot}ZrO_2$; MgO; Ca–ZrO_2	$CaO{\cdot}ZrO_2$
1500	$CaO{\cdot}ZrO_2$; MgO	$CaO{\cdot}ZrO_2$; MgO; Ca–ZrO_2 (traces)	$CaO{\cdot}ZrO_2$
1600	$CaO{\cdot}ZrO_2$; MgO	$CaO{\cdot}ZrO_2$; MgO; Ca–ZrO_2 (traces); $2CaO{\cdot}Fe_2O_3$	$CaO{\cdot}ZrO_2$

the phases with the low temperature melting point were detected – $4CaO{\cdot}Al_2O_3{\cdot}Fe_2O_3$ and $2CaO{\cdot}Fe_2O_3$ (Table 3). It means that at temperatures above 1300 °C, the process of creation and sintering of $CaZrO_3$ was intensified by the presence of the liquid phase. As a result the material with small porosity can be obtained.

Material DI showed a tendency to densification at temperature of 1400 °C. Its shrinkage was rising with the

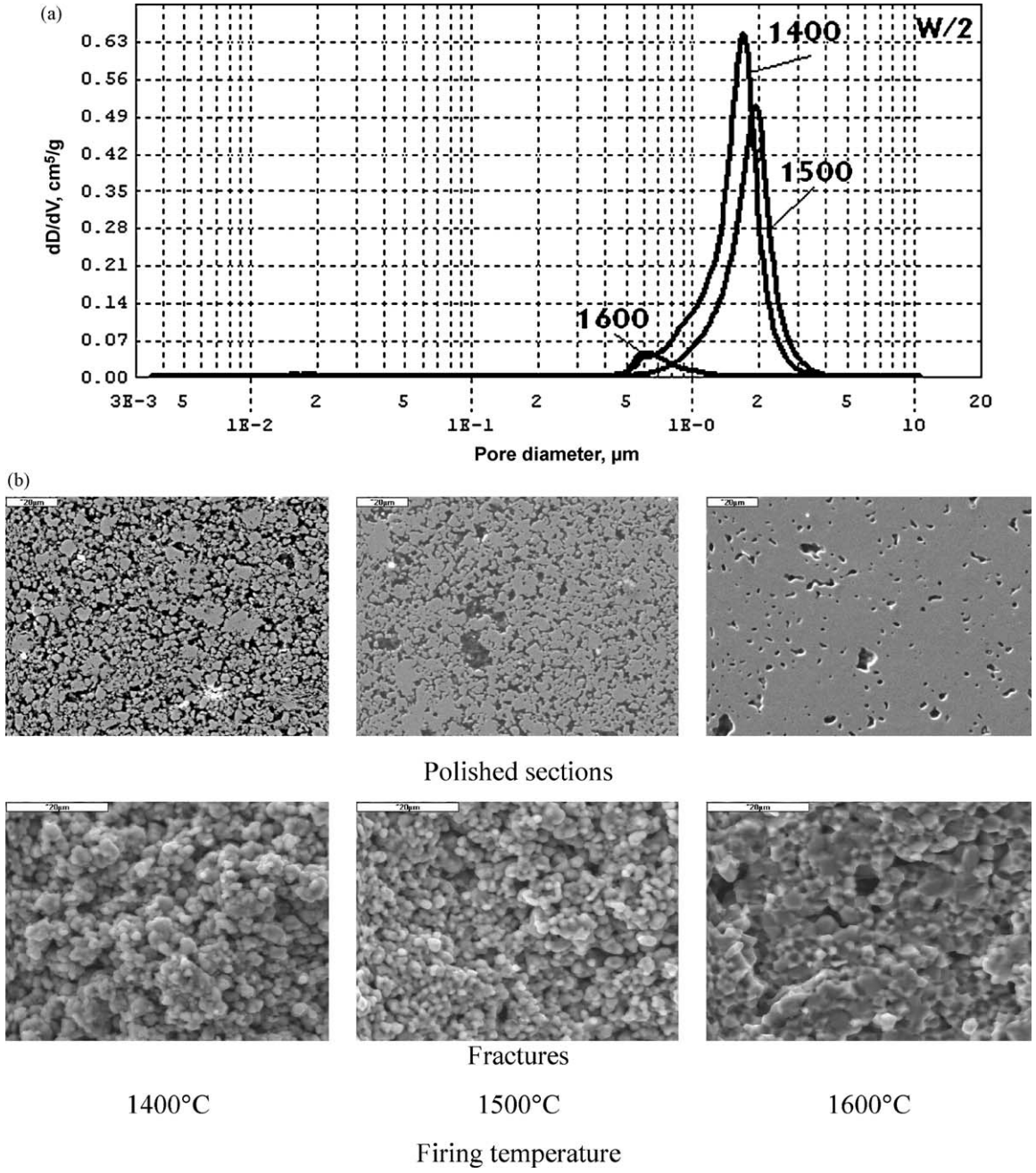

Fig. 13. Pore size distribution (pore frequency curve) (a) and SEM images of microstructure (b) of W/2 material. Bright oval grains – calcium zirconate; dark grey grains – periclase and dark spots – pores.

increase of the firing temperature and was significantly smaller than that recorded for DII material.

Dolomite I has a very small amount of admixtures (~0.1%, see Table 2). The sintering of this material proceeds in the solid state.

W material, made on the base of pure reagents, showed shrinkage at 1600 °C and sintering proceeded in the solid state.

All type of materials (DI, DII and W) during the second step of firing (at temperatures of 1400 °C and higher) showed shrinkage only (Fig. 7). The materials manufactured in two-step process were better densified (see Table 5). The DII/2 material after the second firing showed shrinkage of about 20%, regardless the firing temperature.

The elongation of sintering time up to 5 h caused that the maximum densification of DII/2 material was achieved at 1400 °C and did not change with the increase of sintering temperature. Shrinkage of DI/2 and W/2 materials was increased with the increase of sintering temperature, reaching about 18% at 1600 °C.

Table 5 and Figs. 8–14 show open porosity changes vs. the process type and its maximum temperature. Shrinkage of DI and DII materials sintered in one-step process at 1400–1600 °C range was followed by the significant decrease the pore volume. Bulk density was increased. A similar behaviour was detected for W material at 1600 °C.

Two-step firing of DI/2 and W/2 materials proceeded in a similar way, yet the level of densification was much higher. Densification of DII/2 material was the highest among the investigated materials. The pore volume was <6 mm^3/g, the mean pore diameter was smaller than 0.1 μm and bulk density was between 4.16 and 4.35 g/cm^3. The elongation of the sintering time up to 5 h practically did not change material parameters. Bulk density was about 4.30 g/cm^3 and mean pore diameter was <0.1 μm, regardless the firing temperature.

Two-step firing allowed authors to achieve a better level of densification of all investigated materials then in the materials fired in the one-step process at 1400 °C (Table 5 and Figs. 8–14). An additional treatment (''intermediate calcination'') facilitated obtaining dense MCZ and CZ bodies. The form of such material represented by DII/2 sample achieved the highest density.

The W/2 material after two-step firing is composed only of the $CaZrO_3$ phase. Its density changes depend on maximum firing temperature: 80, 86.7 and 90% of theoretical density (4.95 g/cm^3) for 1400, 1500 and 1600 °C firing temperature, respectively.

Materials of both D series were composed of two phases – $CaZrO_3$ (~82%) and periclase (~16%) showing a significant density difference (4.95 and 3.58 g/cm^3, respectively). The theoretical density of such a mixture amounts to 4.63 g/cm^3. After two-step sintering D materials reached the density as follows: DI/2 – 87.0, 85.5 and 93.5%, DII/2 – 89.8, 95.3 and 94.0%, for 1400, 1500 and 1600 °C firing temperature, respectively.

Scanning electron microscopy images of DI and DII materials fired at temperatures of 1400, 1500 and 1600 °C, by both applied ways, showed mainly oval crystals of calcium zirconate. Periclase crystals were uniformly distributed between them (Figs. 8, 9, 11 and 12). In advance of firing temperature and in the second firing stage, the increase of crystals of both phases, increase of densification and decrease of porosity, were observed. Calcium zirconate crystals reached the maximum size of about 10 μm and periclase crystals were about 20 μm.

SEM images of material W showed in (Figs. 10 and 13) oval grains of calcium zirconate of different sizes. Their size increased with the increase of the firing temperature and in the second firing stage. Simultaneously, the largest pores disappeared and the level of densification increased. The grain rearrangement during sintering led to a significant increase of the interphase contact area.

Table 5
Properties of DI, DII and W materials after firing determined by mercury porosimetry.

Type of material	Firing temperature (°C)	Cumulative pore volume (mm^3/g)		Median pore diameter (μm)		Bulk density (g/cm^3)	
		Firing process		Firing process		Firing process	
		1-Step	2-Step	1-Step	2-Step	1-Step	2-Step
DI	1400	404.0	153.4	3.82	2.50	2.61	4.03
	1500	286.2	48.1	4.18	2.29	2.97	3.96
	1600	125.4	34.5	4.46	0.69	3.10	4.33
DII	1400	69.9	0.3	3.31	0.022	3.42	4.16
	1500	35.2	1.4	2.12	0.007	3.94	4.41
	1600	7.12	5.5	0.04	0.025	4.14	4.35
DII/5	1400	–	5.8	–	0.07	–	4.31
	1500	–	9.9	–	0.03	–	4.35
	1600	–	11.7	–	0.04	–	4.29
W	1400	485.8	138.6	3.13	1.60	2.52	3.95
	1500	489.4	108.3	3.28	1.83	2.42	4.29
	1600	51.1	10.2	3.57	0.68	3.43	4.45

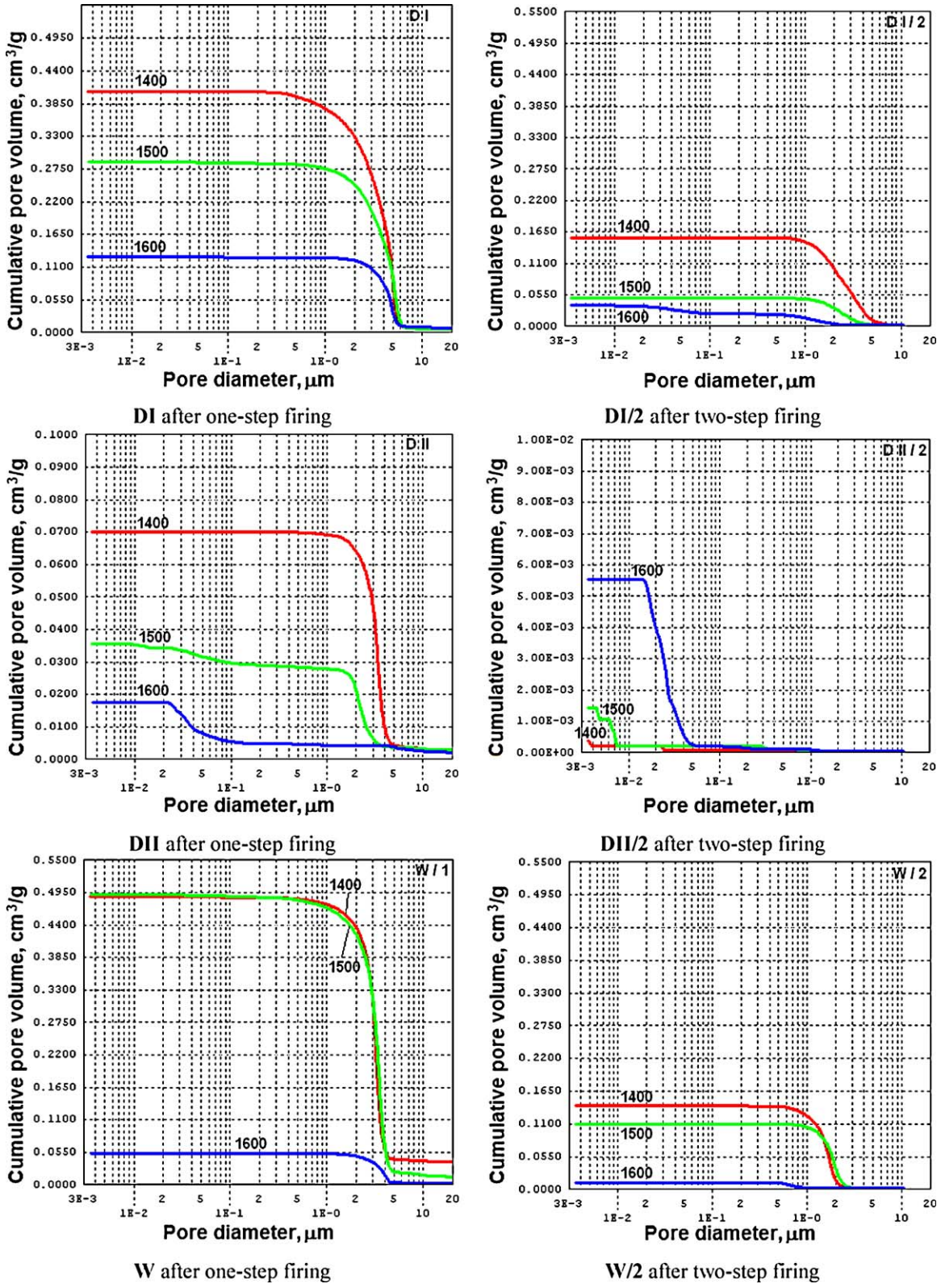

Fig. 14. The cumulative pore volume changes depending on the material type and firing temperature of MCZ (D) and CZ (W) products.

4. Conclusions

The influence of the natural admixtures (SiO_2, Fe_2O_3 and Al_2O_3) content in dolomite raw materials on the microstructure of $CaZrO_3$–MgO materials manufactured in one- and two-step firing processes up to temperature of 1600 °C was investigated.

The synthesis of $CaZrO_3$ in one- and two-step processes was definitely completed at 1500 °C.

The only phase present in the model material synthesized from pure chemical reagents $CaCO_3$ and ZrO_2 after firing at temperature of 1500 °C was calcium zirconate.

In materials synthesized from natural dolomite and ZrO_2 two main phases were present – calcium zirconate and periclase. In $CaZrO_3$–MgO materials achieved at lower temperature, transient phases were present (mainly ferrites and calcium aluminates $4CaO{\cdot}Al_2O_3{\cdot}Fe_2O_3$ or $2CaO{\cdot}Fe_2O_3$). These phases disappeared at higher temperatures. This is probably related to the dissolution of admixtures in the main phases of the $CaZrO_3$–MgO material.

The densification process of investigated materials depended on the presence and amount of admixtures. The level of densification of the model material and the material synthesized from zirconium oxide and dolomite with a small content of admixtures (<0.2%) was increased with the firing temperature; while the material produced from zirconium oxide and dolomite with the higher content of admixtures (∼3.4%) was very dense after firing at 1400 °C and its density did not change significantly with further increase of the firing temperature.

The earlier calcination (the first-step) of the raw mixtures in the two-step firing process lead to obtain dense MCZ and CZ materials. The material obtained from the mixture of zirconium oxide and natural dolomite with the higher admixtures content has the highest densification level (∼95% theoretical density of $CaZrO_3$–MgO) at temperatures of 1500 and 1600 °C.

The longer firing time of this material allowed to achieve dense $CaZrO_3$–MgO material, even at temperature of 1400 °C.

Acknowledgement

The work was partially supported by the grant no. NR15-0014-06 of the Polish Ministry of Science and Higher Education.

References

[1] F. Nadachowski, Outline of Refractory Materials Technology, ŚWT, Katowice, 1995 (in Polish).
[2] H.H. Zender, H. Leistner, H.R. Searle, ZrO_2 materials for application in the ceramics, Interceram 39 (6) (1990) 33–36.
[3] Ch.L. Macey, Refractory solutions for high wear in cement kiln transition zones, in: Proceedings of the 5th UNITECR'97, New Orleans, USA, (1997), pp. 1625–1631.
[4] H. Kozuka, Y. Kajita, Y. Tuchiya, T. Honda, S. Ohta, New kind of chrome-free (MgO–CaO–ZrO_2) bricks for burning zone of rotary cement kiln, in: Proceedings of the 3rd UNITECR'93, Sao Paulo, Brazil, (1993), pp. 1027–1038;
H. Kozuka, Y. Kajita, K. Tokunaga, K. Sakakibara, S. Ohta, Further improvements of MgO–CaO–ZrO_2 bricks for burning zone of rotary cement kiln, in: Proceedings UNITECR'95, vol. 1, Kyoto, Japan, (1995), pp. 256–263.
[5] H. Komatsu, M. Arai, S. Ukawa, Current and future status of chrome-free bricks for rotary cement kilns, Taikabutsu Overseas 19 (4) (1999) 3–9.
[6] J. Ulbricht, W. Schulle, G. Harp, M. Eckert, Chromium-oxide-free basic refractory material for use under severe conditions, Zement Kalk Gips Int. 55 (7) (2002) 70–79.
[7] P. Duwez, F. Odell, H. Frank, F.H. Brown, J. Am. Ceram. Soc. 35 (5) (1952) 109.
[8] T. Igawa, H. Yamamoto, H. Komatsu, M. Matsuzuru, S. Ukawa, Chrome-free bricks with good adhesion of coating in cement rotary kiln, Taikabutsu Overseas 15 (3) (1995) 36–40.
[9] J. Wojsa, J. Podwórny, Z. Patzek, Magnesia-spinel bricks modified with ZrO_2 addition, in: VII-th International Metallurgical Conference, Ustroń-Gliwice, Poland 1997, (1997), pp. 71–76.
[10] H. Komatsu, M. Arai, S. Ukawa, Development of magnesia-spinel bricks with high resistivity against alkali salts in rotary cement kilns, J. Tech. Assoc. Refract. Jpn. 21 (3) (2001) 166–171.
[11] M. Arai, S. Ukawa, The development of chrome free bricks for burning zone of cement rotary kiln, in: Proceedings of the 8th UNITECR'03, Osaka, Japan, (2003), pp. 43–46.
[12] J. Szczerba, Characteristics reaction of magnesia-spinel refractories with kiln hot meal and cement clinker, Ceramika/Ceramics 103 (2008) 543–550.
[13] M. Ohno, K. Tokunaga, Y. Tsuchiya, Y. Mizuno, H. Kozuka, Applications of chrome-free basic bricks to cement rotary kilns in Japan, in: Proceedings of the 8th UNITECR'03, Osaka, Japan, (2003), pp. 27–30.
[14] E. Kawamoto, N. Mimura, K. Shima, M. Loeffelholz, Improvement of MgO–CaO bricks for cement rotary kilns by ZrO_2 addition, J. Tech. Assoc. Refract. Jpn. 23 (4) (2003) 271–275.
[15] S. De Aza, C. Richmond, J. White, Compatibility relationships of periclase in the system CaO–MgO–ZrO_2–SiO_2, Trans. J. Br. Ceram. Soc. 73 (4) (1974) 109–116.
[16] R.K. Ghose, J. White, Trans. J. Br. Ceram. Soc. 79 (6) (1980) 146.
[17] US Patent 4,849,383 (1989).
[18] F. Ozeki, K. Tokanuga, H. Kozuka, Y. Kajuta, T. Honda, Study on refractories affected by utilization of leaping wastes in cement rotary kiln, in: Proceedings of the 7th UNITECR'01, Cancún, México, (2001), pp. 669–684.
[19] S. Radovanovic, The reactions between zirconia from MgO–ZrO_2 refractories and the compounds of Portland cement clinker, in: Proceedings 4th UNITECR'95, Kyoto, Japan, (1995), pp. 224–232;
Reaction behaviour of spinel, zirconia and monocalcium zirconate under working conditions of cement kilns, in: Proceedings 5th UNITECR'97-New Orleans, USA, (1997), pp. 1613–1623.
[20] S. Serena, M.A. Sainz, A. Caballero, Corrosion behavior of MgO/$CaZrO_3$ refractory matrix by clinker, J. Eur. Ceram. Soc. 24 (2004) 2399–2406.
[21] R. Prange, U. Bongers, J. Hartenstein, J. Stradtmann, Present state and future trends in the use of basic refractories in cement and lime kilns, in: Proceedings UNITECR'95, vol. 1, 1995, pp. 248–255.
[22] F. Nadachowski, E. Drygalska, K. Haberko, J. Iwanciw, A. Osiniak, D. Żelazna, A new refractory made by reaction of zircon sand with lime, in: Proceedings UNITECR'93, Sao Paulo, Brazil, (1993), p. 324.
[23] J. Szczerba, E. Drygalska, A. Osiniak, D. Żelazna, Microstructure of dolomite–zircon refractories, Stahl Eisen (Special Issue) (1997) 111–116.
[24] PL Patent 172306 B1 (1997).
[25] PL Patent 178733 B1 (2000).
[26] J.L. Rodriguez, M.A. Rodriguez, S. De Aza, Reaction sintering of zircon–dolomite mixtures, J. Eur. Ceram. Soc. 21 (2001) 343–354.
[27] W.M.N. Nour, A.G.M. Otoman, Shaped basic refractories based on magnesia, limestone and zircon for rotary cement kiln, Ind. Ceram. 27 (1) (2007) 21–28.
[28] R.A. Kordyuk, N.W. Gulko, Dokl. Akad. Nauk SSSR (1962) 639.
[29] K. Niesel, P. Thormann, Tonind. Ztg. 91 (1967) 362.
[30] O. Ruff, F. Bert, E. Stephan, Z. Angor. u. Allgem. Chem. 180 (1929) 219.
[31] R. Angers, R. Tremblay, A.C.D. Chaklader, J. Am. Ceram. Soc. 57 (5) (1974) 231.
[32] B. Phillips, A. Muan, J. Am. Ceram. Soc. 41 (11) (1958) 448.
[33] J.R. Rait, Iron Steel 22 (1949) 186, 91.
[34] B. Philips, A. Muan, J. Am. Ceram. Soc. 42 (9) (1959) 414.
[35] Fig. 3.19, Slag Atlas, 2nd edition, VDEh, Verlag Staleisen GmbH, D-Düsseldorf, 1995.
[36] B. Phlips, S. Somiya, A. Muan, J. Am. Ceram. Soc. 44 (4) (1961) 169.
[37] Schlackenatlas, Verlag Stahleisen mbH, Düsseldorf, 1981 , p. 30 (A. Muan, E.F. Osborn, Phase Equilibria among Oxides in Steelmaking, Addison-Wesley Publishing Company, Inc., Reading, Massachusetts, 1965, p. 45).